Journal of Applied Polymer Science

Thermal and Chemical Stabilization of Ethylene/Vinyl Acetate/Vinyl Alcohol (EVA-OH) Terpolymers Under Nitroplasticizer Environments

Dali Yang,[1] Kevin M. Hubbard,[1] Kevin C. Henderson,[1] Andrea Labouriau[2]

[1]Division of Materials Science and Technology, Polymers and Coatings, Los Alamos National Laboratory, Los Alamos, New Mexico
[2]Division of Chemistry, Chemical Diagnostics and Engineering, Los Alamos National Laboratory, Los Alamos, New Mexico, 87545, USA
Correspondence to: D. Yang (E-mail: dyang@lanl.gov)

ABSTRACT: In this study, we compare the aging behaviors of cross-linked ethylene/vinyl acetate/vinyl alcohol terpolymers, also referred to as EVA-OH, when they are either immersed in nitroplasticizer (NP) liquid or exposed to NP vapor at different temperatures. While thermogravimetric analysis and differential scanning calorimetry are used to probe the thermal stability of aged NP and polymers, Fourier transform infrared, gel permeation chromatography, ultra-violet/vis, and nuclear magnetic resonance are used to probe their structural changes over the aging process. The study confirms that NP degrades through C—N cleavage, and releases HONO molecules at a slightly elevated temperature (<75°C). As these molecules accumulate in the vapor phase, they react among themselves to create an acidic environment. Therefore, these chemical constituents in the NP vapor significantly accelerate the hydrolysis of EVA-OH polymer. When the hydrolysis occurs in both vinyl acetate and urethane groups and the scission at the cross-linker progresses, EVA-OH becomes vulnerable to further degradation in the NP vapor environment. Through the comprehensive characterization, the possible degradation mechanisms of the terpolymers are proposed. © 2014 Wiley Periodicals, Inc. J. Appl. Polym. Sci. **2015**, *132*, 41450.

KEYWORDS: ageing; degradation; EVA-OH; hydrolysis; plasticizer; thermogravimetric analysis (TGA)

Received 20 June 2014; accepted 25 August 2014
DOI: 10.1002/app.41450

INTRODUCTION

In early 2000, a significant amount of effort had been devoted to the degradation study of poly(ester urethane) (referred to as Estane) in a plastic-bonded explosive formulation (e.g. PBX 9501). Many researchers from different DOE facilities (e.g. LANL, SNL, Pantex, and Kansas City Plant) became involved in this effort.[1–7] The important factors to trigger the Estane degradation in the PBX 9501 formula are the presence of moisture and the degradation of nitroplasticizer (NP). NP is an eutectic mixture of bis(2,2-dinitropropyl) acetal (BDNPA) and bis(2,2-dinitropropyl) formal (BDNPF) (50%/50%). Their molecular structures are illustrated in Figure 1. It has been reported that NP undergoes different decomposition pathways when it is thermally treated at low temperature (e.g. 60–75°C)[3] and at high temperature (>160°C), respectively.[4] Instead of forming radicals and NO_2 as occurs at the high temperature condition, a non-radical reaction generates HONO with a low activation energy at the low temperature condition. From their model compounds, Pauler et al. calculated the activation energy of the HONO formation to be <42 kJ/mol. In reality, the activation energy of the NP degradation in a constituent aging study (CAS) was found to be as low as 28 kJ/mol, which suggests that the reactivity of NP can be much higher when it is embedded in a highly heterogeneous matrix with the presence of moisture and other impurities.[3,5,7] It is well known that moisture causes the hydrolysis of the ester group in Estane, and results in chain scission and low molecular weight (M_w) materials.[8] However, due to the thermal degradation of NP, the surrounding environment of Estane becomes acidic, which greatly accelerates the hydrolysis and even the oxidative degradation of Estane.[1,2,6]

Recently, we started the investigation of aging behavior of ethylene/vinyl acetate/vinyl alcohol terpolymer, referred to as EVA-OH [or as vinyl copolymer elastomer (VCE)], which is also used as a binder in filled materials.[9–11] Often, a cross-linked (X-linked or cured) form is used to improve its chemical stability and will be studied here.[12,13] When stored in application systems, it has been reported that EVA-OH slowly uptakes NP from the surroundings.[14–16] Therefore, this material is essentially exposed to similar conditions as Estane. Figure 2 illustrates the molecular structures of EVA-OH and Estane that have the same functional groups, but different chain conformations. Therefore, it is reasonable to predict that the degradation mechanisms occurring in Estane will happen to EVA-OH as well. Now, the question arises as to why Estane is unstable, but the

© 2014 Wiley Periodicals, Inc.

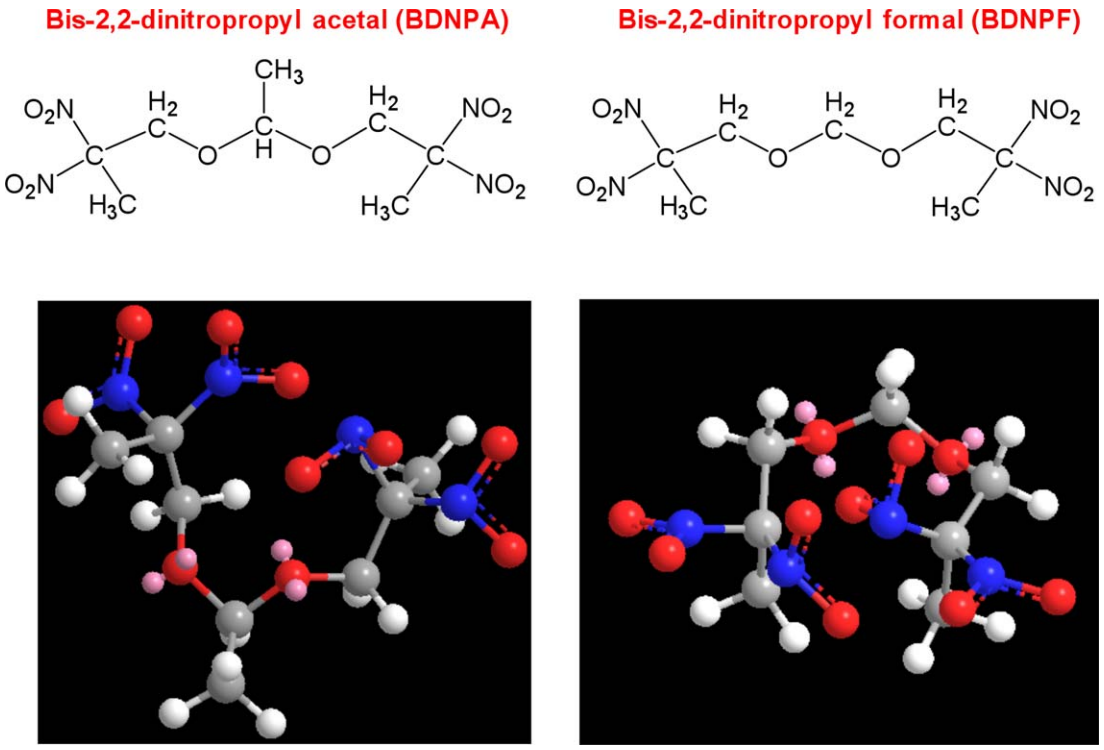

Figure 1. The molecular structures of BDNPA and BDNPF. NP is an eutectic mixture of these two components (50%/50% mixture). [Color figure can be viewed in the online issue, which is available at wileyonlinelibrary.com.]

aging of EVA-OH at low temperature (<75°C) is rarely reported.[11] The different stabilities of these two polymers ought to be directly related to how they have been used. In Table I, we compare their application conditions. When Estane is used as a binder in the PBX 9501 formula, it is mixed together with 95 wt % HMX and 2.5 wt % NP. The polymer concentration is

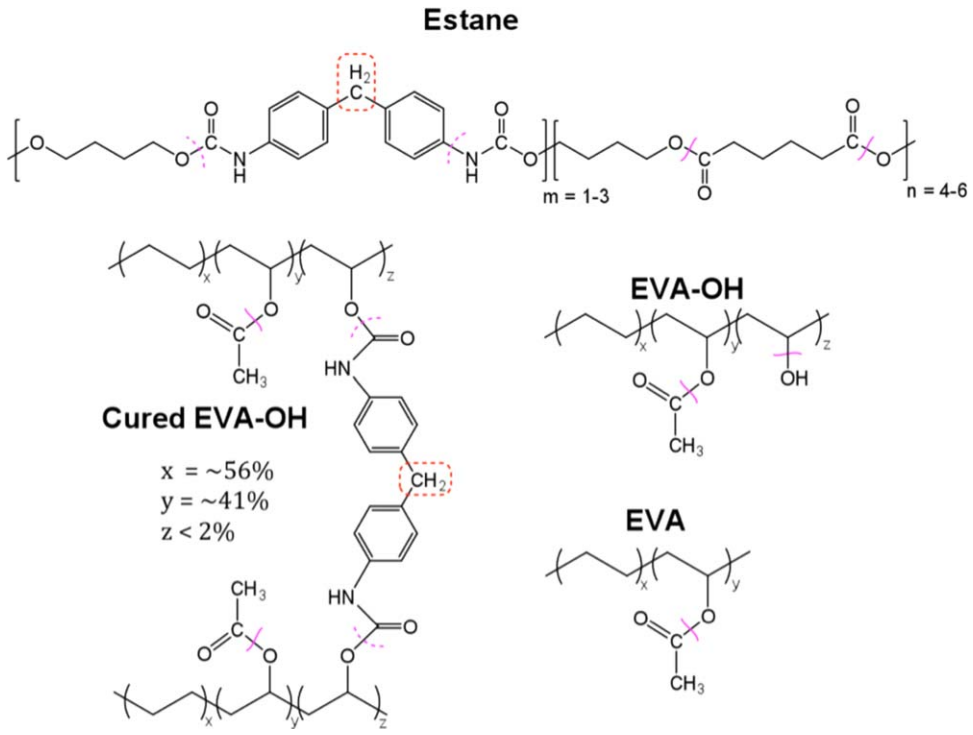

Figure 2. The molecular structures of Estane, cured EVA-OH, EVA-OH, and EVA (functional groups in which the degradation likely occur are indicated). The cured EVA-OH is used in this study. [Color figure can be viewed in the online issue, which is available at wileyonlinelibrary.com.]

Table I. Comparison of the Usage and Exposure Environment of Estane and EVA-OH in Application Systems

	Estane	Cured EVA-OH
Conc. (%)	2.5	>10
Exposed to	NP, moisture	NP, moisture
Temperature (°C)	<40	>40
NP and moisture source	direct	indirect
Anti-oxidant	Irganox	No
Aging problem	Yes	No report

as low as 2.5 wt %. The large interfacial area between Estane and HMX particles significantly enhances the kinetics of the interaction between polymer and other molecules in the formula.[7] Further, NP and/or moisture are readily available inside the PBX 9501 formula, and thus the aging process starts at the beginning of the Estane application. On the contrary, when EVA-OH is used as a binder in the filled composites, it is used in the X-linked form, and its concentration is higher. Although there is some interfacial area between EVA-OH and filler particles, this area is less than that in the PBX 9501 formula. Furthermore, NP and/or moisture are initially not present in the composite. From the previous studies, we confirm that it will take at least a few years for NP to migrate into the EVA-OH domain. Therefore, all of these factors significantly reduce the degradation rate of the EVA-OH in its application, and result in a long time delay to observe the aging signs of EVA-OH. Furthermore, due to their different chain conformations, the hydrolysis in Estane results in the chain scission in the backbone, which causes the low MW materials and poor mechanical integrity.[17] On the contrary, the same hydrolysis in EVA-OH mainly causes the scission in —CO— of vinyl acetate (VAc) and urethane groups in the X-linker, which does not break the backbone of EVA-OH. Therefore, at least at the early stage, the impact of the EVA-OH degradation on the M_W is not as significant as that on Estane. However, once the X-linker is broken down, uncured EVA-OH will become more vulnerable to further degradation. For the oxidative degradation, compared to Estane, the EVA-OH/filler composite has a disadvantage because it lacks an anti-oxidant (e.g. Irganox) in the matrix. Hence, in addition to the hydrolysis, the oxidants (NO_x) and water generated from the NP degradation will readily attack EVA-OH.

For the clarity of our discussion, in Figure 2, we also include the molecular structure of uncured EVA-OH and EVA (the copolymer of ethylene and VAc). Clearly, the main structure of uncured EVA-OH is almost the same as that of EVA. The thermal aging of EVA at the high temperature (>200°C) has been well studied.[11,18–24] Researchers concluded that the deacetylation typically occurs at the first degradation and results in the loss of acetic acid and unsaturated materials. However, in this study, we will focus on the aging behavior of EVA-OH at low temperature (<75°C), but with the presence of NP and filler particles. When NP migrates into the EVA-OH domain, we are not sure whether NP molecules transfer into the EVA-OH matrix in its liquid and/or vapor phases. However, it is expected that the NP vapor pressure will build up to establish equilibrium with its liquid phase. Therefore, it is important to understand how EVA-OH interacts with NP liquid and vapor, respectively. In the previous study, we have demonstrated that the heterogeneity of the EVA-OH/filler composites significantly changes the NP transport properties and we expect a great impact in the aging behavior of EVA-OH.[16] Here, we will use 20% EVA-OH/filler composites as a model compound to conduct the aging study.

EXPERIMENTAL

EVA-OH Sample Preparation

The EVA-OH composites were prepared at Honeywell's Kansas City Plant. The manufacturing process involves the controlled hydrolysis of EVA to give the ethylene/vinyl acetate/vinyl alcohol terpolymer (uncured EVA-OH). The uncured EVA-OH and curing agent diphenyl-4,4′-methylenebis(phenylcarbamate) (Hylene MP) are compounded together to form the cross-linked form, as illustrated in Figure 2. The approximate fractions of the three segments in the cured EVA-OH (herein simply called EVA-OH) are given in Figure 2. EVA-OH. For the filled EVA-OH, filler particles are added during the compounding process. The filled EVA-OH elastomer is referred to as the EVA-OH composite. NP is obtained from Pantex. More description about these materials can be found elsewhere.[11,13,16,25]

Six sets of the EVA-OH composites were kept in three containers, which were aged at room temperature (RT), 50, and 75°C, respectively. Two sets of the EVA-OH samples were kept in the same container in which one set was immersed inside NP liquid and the other set was kept in the headspace and exposed to NP vapor. Both liquid immersed and vapor exposed samples were periodically removed from the container for the thermal and chemical characterization. Due to the sample removal, and ongoing characterization of the NP liquid and aged EVA-OH samples, we opened the containers from time to time. Therefore, a headspace analysis was not designed in this study. Before the aging experiments, the containers were purged with nitrogen. The sample removal was conducted inside the nitrogen glove box to minimize the oxygen exposure, and was conducted in the way to minimize the operation time.

Thermal Analysis

Thermal Instruments Q500 Thermogravimetric Analyzer (TGA) was used to analyze the thermal stability of NP and EVA-OH samples. The samples, with a size of ~25 mg, were heated from ambient temperature to 600°C at 10°C/min with a nitrogen purge (10 mL/min). Platinum pans were used in the TGA measurement. DSC, with a sample size of ~25 mg, was carried out using a TA Instruments Q2000 Modulated Differential Scanning Calorimeter from −85 to 140°C at 10°C/min heating rate. The temperature was controlled using a refrigerated cooling accessory (RCA90). The flow rate of nitrogen purge was 50 mL/min. The samples were encapsulated in aluminum Tzero® pans. The instrument was calibrated with indium and sapphire standards.

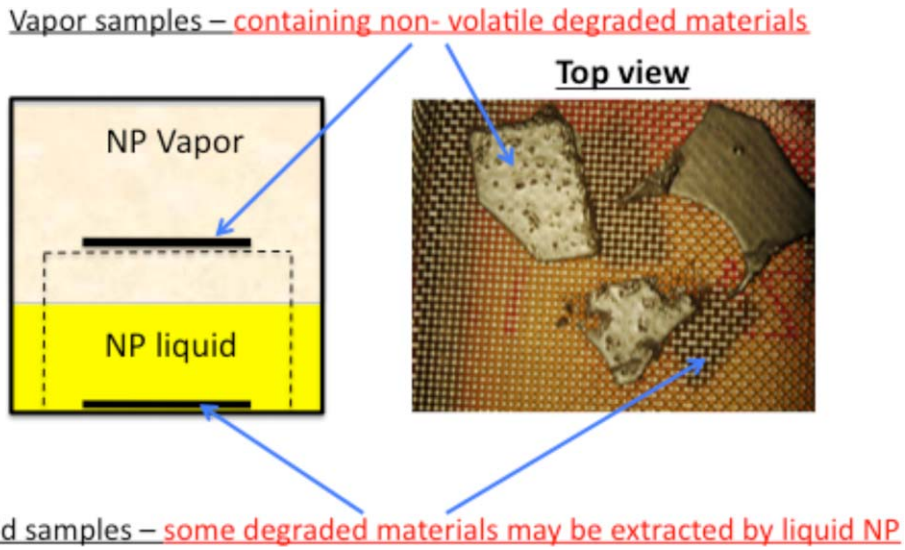

Figure 3. Illustration of the physical appearance of the EVA-OH composites exposed to NP vapor at 75°C for 9 months. [Color figure can be viewed in the online issue, which is available at wileyonlinelibrary.com.]

Fourier Transform Infrared (FTIR) Spectroscopy

FTIR absorption data were obtained with a Nicolet 6700 FTIR bench operating in Attenuated Total Reflectance (ATR) mode. Data were collected using a Spectra-Tech Thunderdome ATR accessory equipped with a germanium crystal. All data were taken with a resolution of 4 cm^{-1}, and represent the average of 120 scans.

Gel Permeation Chromatography (GPC)

Two GPC systems were used. Agilent PL GPC-220 consists of a differential refractive index (DRI) detector and Agilent PLeg Mixed C and Mixed D columns (7.0 × 300 mm–diameter × length). The injection volume was 100 μL with a flow rate of 1.0 mL/min. Polymer MWs were calculated based on the DRI signal against polystyrene standards (Agilent, EasiCal PS2AB). Agilent Cirrus software was used to reduce the data. Waters GPC consists of an Alliance 2690 pump, a Waters 996 photodiode array (PDA) detector, and Agilent PLeg mini-Mixed C and Mixed D columns (3.6 × 250 mm). The injection volume was 50 μL, and the effluent flow rate was 0.3 mL/min. The Waters GPC was mainly used to retrieve the UV/vis spectra of the eluded fragments of aged samples. The columns in both systems were heated to 40°C. The EVA-OH samples were prepared based on the polymer concentration of 1 mg/mL in anhydride THF (Aldrich, HPLC grade containing a 250 ppm of BHT). The liquid NP solution was made at ~1 mg/mL. All solutions were kept at 50°C for overnight. The solutions were filtered through a 0.45 μm Teflon filter prior to injection.

^{13}C Nuclear Magnetic Resonance (NMR)

Solid-State ^{13}C Magic Angle Spinning Nuclear Magnetic Resonance Spectroscopy (MAS NMR) was obtained in a Bruker 400 MHz spectrometer operating at 100.62 MHz. A 4 mm MAS probe was used. Spectra were obtained using direct detection with a pulse of 4.0 micro-sec and a delay time of 20 sec and about 10K scans. Tetramethylsilane (TMS) was the external reference.

RESULTS AND DISCUSSION

Physical Appearance of Aged EVA-OH Samples

Figure 3 presents the photos of the EVA-OH samples exposed to NP vapor at 75°C for 9 months. After aging, the samples exposed to the NP vapor (referred to as the vapor sample) are completely deformed. The sample surface fills with bubbles, which indicates outgassing during the degradation process. The polymer becomes saggy and completely loses its mechanical integrity. On the contrary, the sample immersed inside the NP liquid (referred to as the liquid sample), as blue arrows pointed in Figure 3, preserved its physical appearance well. The results suggest that although both sets of samples were thermally aged at the same temperature and for the same period of time, they degraded very differently.

NP Uptake in the EVA-OH Composites

In Figure 4, we compare the isotherms of NP uptake as a function of time when the EVA-OH composites were exposed to NP liquid and vapor, respectively. As expected, the liquid samples uptake NP at a much faster rate than the vapor samples. At RT, the NP isotherm of the liquid sample needs more than 9 months to reach a plateau. At 75°C, the NP isotherm reaches a plateau within a couple of days, holds a constant mass for more than 3 months, and then starts to increase again. This extra weight gain may be an indication of the degradation of NP and/or EVA-OH. The isotherm at 50°C sits between RT and 75°C isotherms. Since this temperature is very close to the softening/melting point (T_m) of the VAc segment in EVA-OH, the prolonged heating not only gradually changes the morphology of the composites and enhances the mobility of the polymer, but also increases the mobility of NP. Therefore, the NP uptake increases. Eventually, the prolonged heating may also trigger the degradation of NP and thus the possible degradation of EVA-OH. All of these factors complicate the

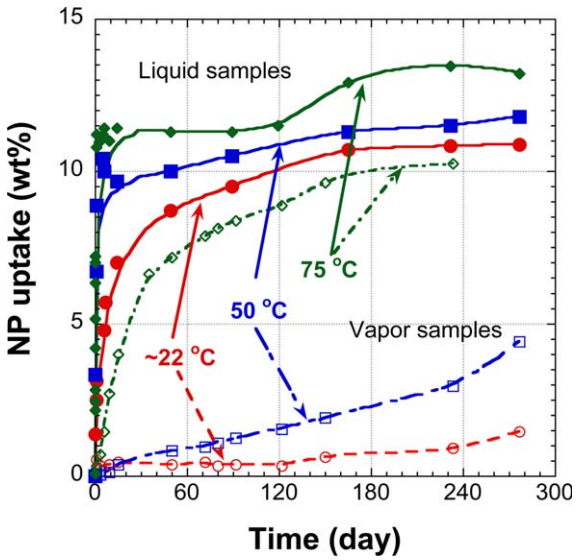

Figure 4. The comparison of the NP uptake by the EVA-OH composites at different temperatures and times when the samples were immersed in the NP liquid and exposed to the NP vapor (after 9 month exposure, we were not able to detach the 75°C samples from substrate without substantially losing some sample mass, as illustrated in Figure 3) (NP uptake is calculated based on the pristine sample weight). [Color figure can be viewed in the online issue, which is available at wileyonlinelibrary.com.]

50°C isotherm. As a result, its isotherm does not reach a plateau over the 9 month heating course.

On the other hand, the vapor samples uptake NP at very different rates, which highly depend on the temperature. At RT, due to the low vapor pressure of NP,[4] the vapor sample only gains <2 wt % after the 9 month exposure. The 50°C exposure slightly increases the rate of NP uptake. The 75°C exposure greatly accelerates the rate of NP uptake because of the largely increased vapor pressure of NP,[4] which allows a higher NP concentration gradient to build around the EVA-OH samples. The high temperature also softens the polymer matrix. Both factors enhance the mobility of NP molecules inside the EVA-OH composites, and increase the NP diffusion process. At 75°C, the NP uptake greatly increases within the first 2 months and then slows down. The slow weight gain at the later portion of the isotherm may be attributed to the degradation of NP and EVA-OH, and is the combination of out-gassing together with NP uptake. After 9 months, the vapor samples were firmly stuck to their stainless steel mesh supports, and were impossible to remove for an accurate weight measurement.

EVA-OH Aged Inside the NP Liquid

Thermal Analysis. Figure 5 presents the TGA results of the EVA-OH composites before and after the NP immersion at different temperatures for 9 months. Typically, the pristine EVA-OH has two peaks on the 1st derivative of weight loss with respect to temperature (referred to as $DT_{EVA\text{-}OH}$), which are related to the polymer thermal decomposition. The first peak (347.3°C) is associated with the decomposition of VAc group along the backbone to form acetic acid, while the second peak (461.4°C) is due to the thermal decomposition of all hydrocarbon functional groups in the polymer.[11,26]

When EVA-OH is immersed inside the liquid NP at RT, NP molecules slowly diffuse into the EVA-OH matrix, but do not noticeably change these two $DT_{EVA\text{-}OH}$s of the polymer. On the other hand, as discussed below, the 1st derivative of the weight loss of NP against temperature (DT_{NP}) in the range of 30–270°C changes appreciably. NP is an eutectic mixture of BDNPA and BDNPF (50%/50%). Both compounds by themselves are solid at the ambient conditions. Their TGA results, in Figure 6, show that the DTs of BDNPA and BDNPF are 239.3 and 246.9°C, respectively. However, NP—the 50%/50% mixture of BDNPA and BDNPF, is a liquid at the ambient conditions with a melting point of −15°C,[27,28] and only gives one DT_{NP} at

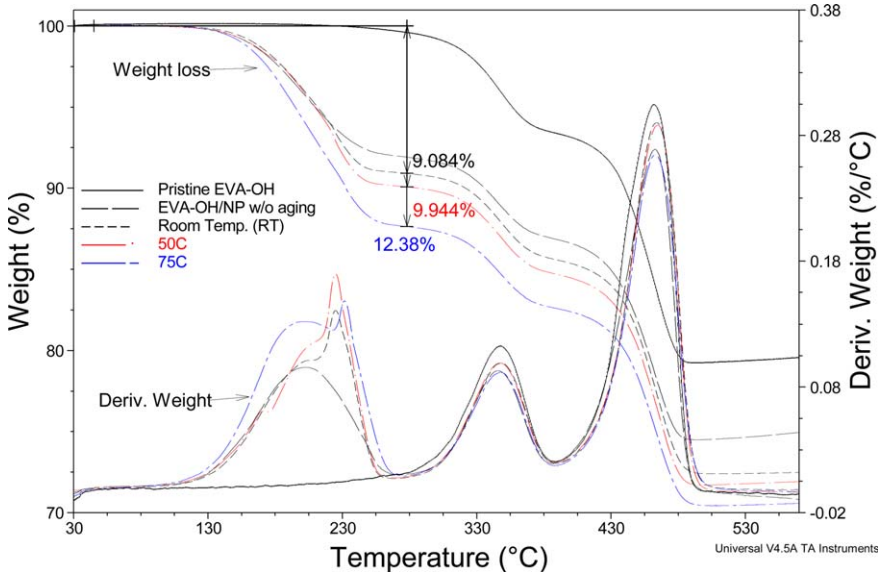

Figure 5. TGA results of the EVA-OH/filler/NP composites before and after the NP immersion for 9 months at different temperatures. [Color figure can be viewed in the online issue, which is available at wileyonlinelibrary.com.]

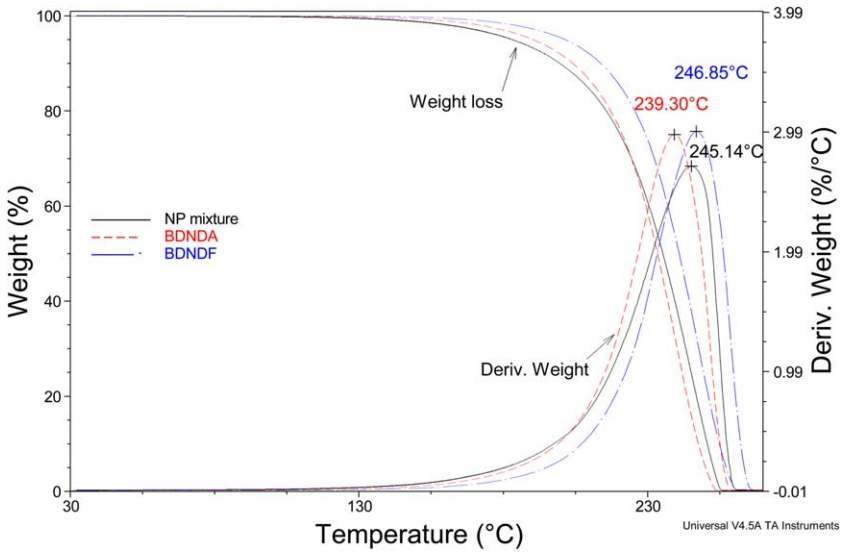

Figure 6. TGA results of NP mixture, BDNPA, and BDNPF. [Color figure can be viewed in the online issue, which is available at wileyonlinelibrary.com.]

245.1°C. However, when the NP molecules diffuse inside the EVA-OH/filler matrix (w/o aging), its DT_{NP} decreases to 202.5°C, as shown in Figure 5. This large decrease in DT_{NP} (>35°C) suggests that the interaction between NP and EVA-OH is weaker than that among NP molecules.[16] The composite matrix provides effective diffusion channels and allows the NP liquid to evaporate from the matrix at a faster rate compared to the evaporation from free NP liquid. As the immersion extends to 9 months at RT, the NP uptake in the EVA-OH composites increases from 8.04 to 9.08 wt %. Simultaneously, the DT_{NP} increases to 224.5°C (as shown in Figure 5), but also includes a shoulder on the low temperature side. We believe that as the diffusion reaches an equilibrium stage, the interaction among NP and EVA-OH molecules adopts the lowest energetic state. In addition to some free NP accumulated in the voids in the EVA-OH matrix,[16] multiple layers of NP may cover the sorption sites. Both factors allow NP to evaporate and decompose in a way that more resembles the free NP liquid. On the other hand, this deformed DT_{NP}, a peak with a shoulder, suggests that the two components in the NP mixture (BDNPA and BDNPF) might interact with EVA-OH differently. The difference between BDNPA and BDNPF might come from their steric structures. Without an extra methyl group, BDNPF might have better flexibility to access into the polymer domain whereas BDNPA may have a weaker interaction with EVA-OH, giving the low temperature shoulder.

For the 50°C sample, except for the increased NP uptake, its TGA result is similar to the RT sample. However, as the immersion temperature increases to 75°C, the shoulder in the DT_{NP} curve develops to a separate peak at ~200°C, and the original peak at 224.5°C shifts to a higher temperature of 231.3°C. These results might indicate that the different affinity between BDNPA and BDNPF toward EVA-OH becomes even more pronounced. Since BDNPA has a higher vapor pressure at the temperature >56°C,[4] the low temperature DT_{NP} (~200°C) is most likely associated with BDNPA whereas the high temperature DT_{NP} (~224.5°C) might be associated to BDNPF.

In Table II, we summarize the weight loss of the samples at different temperature ranges, composition of EVA-OH in its composites, and estimated VAc content in EVA-OH. For the pristine EVA-OH, the weight loss below 277°C (the 1st weight loss) is

Table II. Summary of Weight Loss at Different Temperature Ranges for the EVA-OH Composites Before and After the NP Liquid Immersion at Different Times and Temperatures

	Wt loss (%) at different temp. ranges			Polymer[a]	
Sample	1st <277°C	2nd 277–390°C	3rd 390–500°C	(wt %)	VAc (%)[a]
Pristine	0.79	5.79	13.55	20.4	41.1
RT (w/o aging)	8.04	5.04	12.42	19.5	41.2
RT (9 months)	9.08	5.40	13.17	19.7	43.1
50°C (9 months)	9.94	5.39	12.97	19.0	45.1
75°C (9 months)	12.38	5.01	12.19	17.8	46.1

[a] We assume that the weight loss of the sample between 277 and 500°C is due to the polymer decomposition. With this assumption, we calculate the polymer weight (wt %) in the sample. The content of VAc in the EVA-OH polymer is calculated based on the weight loss between 277 and 390°C. The same methodology is applied for the NP vapor exposed samples.

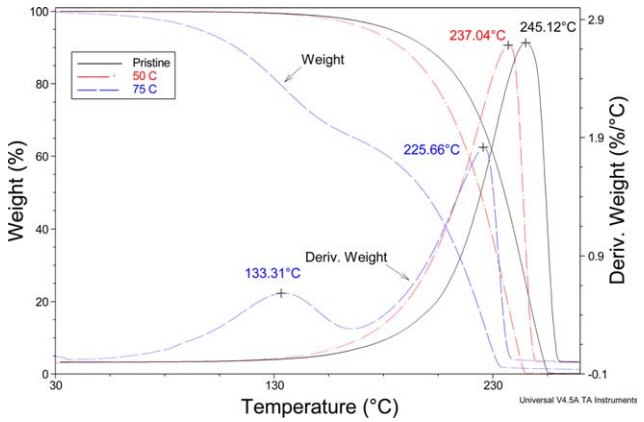

Figure 7. The TGA results of liquid NP before and after EVA-OH immersion at different temperatures for 9 months. [Color figure can be viewed in the online issue, which is available at wileyonlinelibrary.com.]

minimal, and corresponds to a trace amount of un-reacted X-linker and impurities. The weight loss between 277 and 390°C (the 2nd weight loss) is associated with the thermolysis of the VAc segment, which releases acetic acid. Based on the MW ratio of acetic acid (60.05 g/mol) to the monomer of VAc (86.09 g/mol), we estimate a content of 41.1% of VAc in the EVA-OH polymer. The results are similar to the literature values.[11] At RT, the saturation of NP in the EVA-OH composite usually takes a couple of months. We treat this kind of sample as an "non-aged". Its 1st weight loss is associated with the NP evaporation/decomposition, and typically <8.5 wt % for the 20% EVA-OH/filler composite.[16] The short term NP immersion does not noticeably change their TGA results. After the 9 month immersion, the NP uptake reaches its saturation with the slightly increased 1st weight loss of 9.08%. The VAc content in the 9 month aged sample (43.1%) is slightly higher than that in the pristine (41.1%), and non-aged EVA-OH/NP (41.2%) samples. This may be due to the more thorough extraction of un-reacted X-linker and impurity from the polymer matrix, which reduces the total polymer weight and accordingly gives a slightly increased VAc content. As the temperature increases from RT to 50°C, the 1st weight loss of the aged sample increases from 9.08% to 9.94%, which is mainly due to the increased NP uptake, compared to the RT sample. The polymer concentration is similar to the RT samples with a slightly increased VAc content, which might be due to the further extraction of un-reacted X-linker and/or the possible polymer degradation. After aging at 75°C for 9 months, the 1st weight loss further increases to 12.4%. Accordingly, the VAc content in the polymer increases to 46.1%. The large changes in the TGA results indicate some degradation of NP and/or EVA-OH, which will be verified in the later sections.

Figure 7 presents the TGA results of the NP before and after the EVA-OH immersion. The used NP at the RT immersion gives an almost identical TGA result (not shown) as the pristine NP does. After being used for the EVA-OH immersion at 50°C for 9 months, the DT_{NP} of this used NP slightly decreases from 245.1 to 237.0°C, which suggests that the prolonged heating at 50°C slightly decreases the NP stability. As the temperature increases to 75°C, the DT_{NP} further decreases to 225.7°C, which confirms the significant degradation of NP. Simultaneously, a broad peak is detected between 40 and 160°C with a peak at 133.3°C, which might be associated with the dissolution of the fragments extracted from the degraded materials.

For the same set of EVA-OH/NP samples, we conducted the DSC analysis and summarized the results in Table III. Since the pristine EVA-OH consists of ~56% ethylene, ~41% VAc, and <2.0% VA, its thermal properties is dominated by the first two of these components. The glass transition temperature (T_g) of polyethylene (PE) ranges from −120 to −25°C (depending on its density) while the T_g of polyvinylacetate (PVAc) is ~30°C.[26,29] Here, the T_g of pristine EVA-OH is ~ −35°C. Typically, EVA-OH softens as the temperature rises above room temperature, and starts to melt at 54.6°C, which is much lower than the melting point (T_m) of PE (between 95 and 140°C). This T_m may be due to the melting of VAc segments in the EVA-OH with some influence of its T_g.[13] Correspondingly, the heat of fusion of this peak is 13.46 J/g (calculated based on the polymer weight) for the pristine EVA-OH composite. The 9 months aging at RT slightly decreases both T_g and T_m of the sample. Accordingly, the heat of fusion decreases from 13.47 to 11.93 J/g. Due to the affinity between NP and EVA-OH, NP acts as a plasticize of polymer. Since the plasticization mainly takes place in the amorphous phase of polymer, which causes the characteristic effect of lowing the T_g. However, the effect of a plasticizer on the crystallinity of a polymer is complicated. The crystallinity of the polymer can be increased or decreased by the plasticizer depending on many factors, such as interaction strength (chemical vs. physical) between plasticizer and polymer, temperature difference between experimental conditions and melting point of polymer, heterogeneity of the samples and so forth.[30] Since the liquid immersion EVA-OH sample here was fully saturated with NP, the NP concentration in polymer domain is more than 40%. As the polymer chains become more solvated after a long time interaction, the physical interaction between NP and EVA-OH may disrupt the physical interaction between polymer chains and slightly decrease its crystallinity. It is a most likely case for the RT samples because the chemical characterizations do not suggest appreciable degradation of the polymer (see later sections). As temperature increases to 50°C, the further decreased T_g and heat of fusion

Table III. Summary of the T_g, T_m, and Heat of Fusion of the EVA-OH Samples Before and After the NP Liquid Immersion at Different Temperatures for 9 Months

Sample	T_g (°C)	T_m (°C)	H (J/g—polymer)[a]
Pristine	−35	54.6	13.47
RT (9 months)	−36	52.7	11.93
50°C (9 months)	−37	53.9	9.28
75°C (9 months)	−39	47.8	5.73

[a] The polymer weight in the composites is estimated based on the TGA results. The heat of fusion is calculated base on the polymer weight. Here, we only use this value for the comparison purpose, but not use for the crystallinity calculation. The same methodology is applied for the NP vapor exposed samples.

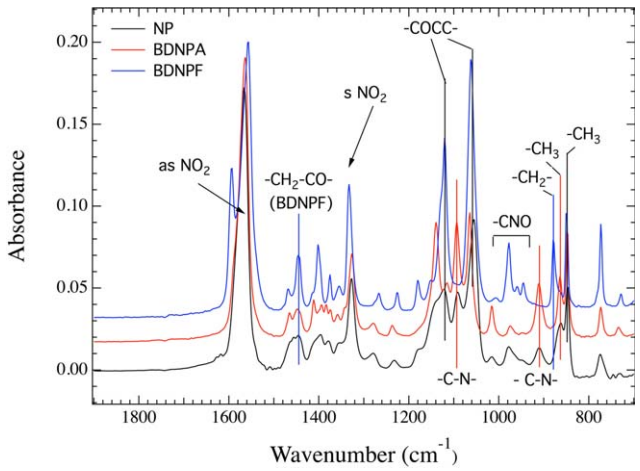

Figure 8. FTIR spectra of NP (an eutectic mixture of BDNPA and BDNPF), BDNPA, and BDNPF. [Color figure can be viewed in the online issue, which is available at wileyonlinelibrary.com.]

of the aged sample may be also due to the polymer degradation in addition to the NP plasticization. As the temperature further increases to 75°C, the T_g, T_m, and heat of fusion for the aged sample significantly decrease. Similar to the TGA results, these large changes indicate noticeable degradation of polymer, such as chain scission.

Structural Characterization. Figure 8 presents the FTIR spectra of pristine NP and the two components (BDNPA and BDNPF) in the NP mixture. The only difference between BDNPA and BDNPF in their molecular structures is the extra —CH_3 group in the center of the BDNPA molecule, as shown in Figure 1. Due to their structural similarity, many major peaks, such as asymmetric and symmetric —NO_2, —CCOC—, —CH_n, simply overlap in the NP spectrum. However, the structural difference does bring some unique peaks for the individual molecule. For example, BDNPF gives different absorption features at —CH_2—CO—, —CNO, and —CH_2— at 1420, 1200–900, and 870 cm^{-1}, respectively. Without the —CH_3 group, the two —COCC— absorption features in BDNPF are much stronger than these in BDNPA. On the other hand, BDNPA gives different features for —C—N— (at 1090 and 910 cm^{-1}) and —CH_3 (at 860 cm^{-1}), respectively. We can use these peaks to detect their presence in the samples.

Figure 9 presents the FTIR spectra of the NP before and after the EVA-OH immersion for 9 months at different temperatures. For better illustration, the spectra are divided into two regions. The FTIR spectrum of the 50°C NP is very similar to the one for pristine NP, which confirms that this temperature does not cause the significant degradation of NP. On the other hand, several new peaks, free —OH (3580 cm^{-1}), —OH (from —OOH group), >NH, —NH_2, ar—CH— and ar—C=C, and —C=O, appear in the 75°C NP sample. The —OH (from —OOH) and >C=O (at 1740 cm^{-1}) groups suggest the presence of acetic acid.[23] Since the >NH, —NH_2, and >C=O groups are typically generated from the NP degradation at high temperature (>160°C),[3] and the aromatic groups can only come from X-linkers, the newly formed amine and aromatic products are most likely from the X-linker molecules that were extracted into NP liquids from the degraded EVA-OH samples during the immersion process. The disappearance of the 1090 cm^{-1} peak and reduced intensity of the 910 cm^{-1} peak, associated with —C—N— stretching from BDNPA, suggests that the NP degradation may be caused by the cleavage of —C—N— bonds in BDNPA.

Since a noticeable degradation of NP occurs at 75°C, we will focus on this temperature, but at different aging times, as shown in Figure 10. Compared to the FTIR spectrum of pristine EVA-OH, the major spectral changes in the 5 month sample are due to the NP uptake. As the sample was further aged up to 9 months, additional spectral changes are observed. The increased NO_2 intensity suggests the higher NP content. Additionally, the newly detectable —OH (from —OOH group at 3430 cm^{-1}) and slightly broader >C=O feature (at 1740 cm^{-1}) confirm the acetic acid and ketone formation. The newly detected >NH and —NH_2 groups (at ~3200 cm^{-1}) and the ar—CH— (from the aromatic rings) and =CH— groups (at 3020 cm^{-1}) suggest that we might be detecting free molecules with structures similar to the X-linker molecules. Furthermore, the slightly reduced intensities of the —CO— peaks at 1740, 1240, and 1010 cm^{-1}, and —CH=CH— peaks at ~970 cm^{-1}, may be due to the removal

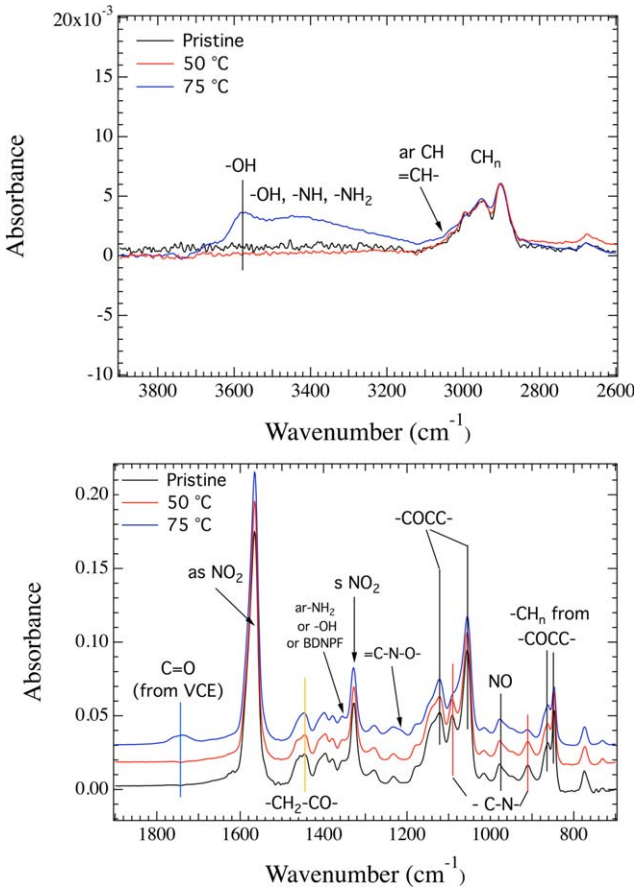

Figure 9. FTIR spectra of the liquid NP before and after the immersion experiment at 75°C for 9 months. [Color figure can be viewed in the online issue, which is available at wileyonlinelibrary.com.]

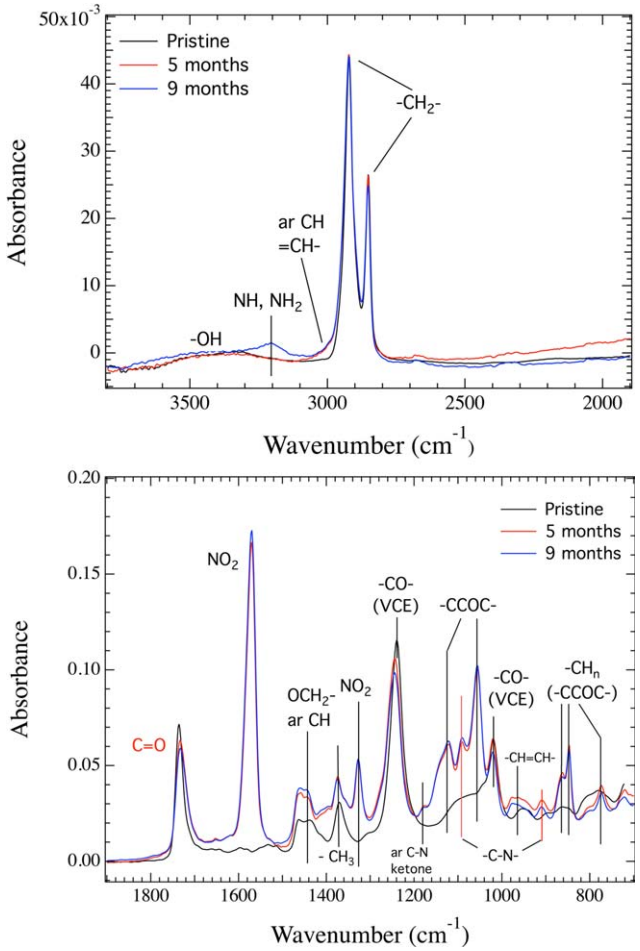

Figure 10. FTIR spectra of the EVA-OH composites before and after NP liquid immersion at 75°C. [Color figure can be viewed in the online issue, which is available at wileyonlinelibrary.com.]

of the formed acetic acid and scission products of X-linkers from the degraded materials into liquid NP.

In summary, NP is relatively stable when it is thermally treated at 50°C for 9 months. However, as the temperature increases to 75°C, NP starts to degrade after the 9 month heating. The TGA and FTIR results suggest that the NP degradation occurs in BDNPA, and also accelerates the EVA-OH degradation, which might occur in both VAc and urethane groups. As a result, acetic acid is generated and the X-linker is incised from the EVA-OH main chains, which changes the chemical structures of EVA-OH.

EVA-OH Aged in the NP Vapor

FTIR Spectroscopy. Figure 11 presents the FTIR spectra of the EVA-OH samples before and after exposure to NP vapor for 9 months. At RT, the peaks associated with NP are small, which confirms the minimal NP uptake in the EVA-OH polymer. Except for that, the aged sample gives the spectrum similar to the pristine EVA-OH. At 50°C, the larger NO_2 peaks confirm the increased NP uptake. Additionally, a broad band related to —OH and —NH— starts to emerge in the region of 3800–3200 cm^{-1} and the >C═O peaks at 1710 and 1180 cm^{-1} become broader, which suggest the formation of alcohol and ketone groups. The intensities of the >C═O peak at 1740 cm^{-1} and —C—O— peak at 1240 cm^{-1} decrease, which may be due to the evaporation of the formed acetic acid. The changed spectrum suggests that EVA-OH degradates at a temperature as low as 50°C in the NP vapor. At 75°C, the FTIR spectrum of the aged EVA-OH completely changes in the entire region. In the region of 3800–3200 cm^{-1}, two new peaks evolve from the broad band, which are related to the —NH— stretch with and without H-bonding interaction, and the formation of polymeric alcohols (—OH) and/or —OOH (from acetic acid), respectively.[23] The shoulder (at 3010 cm^{-1}) associated with ar—CH and ═CH— further grows. The intensity ratio between the asymmetric and symmetric —CH_2— stretching changes as well. In the region of <2000 cm^{-1}, the peaks at 1570 and 1330 cm^{-1} related to the —NO_2 greatly increase because of the increased NP uptake. However, the temperature impact is more than simply an increase in the NP uptake. As the intensities of two characteristic peaks of EVA-OH (—C═O at 1740 and —C—O— at 1240 cm^{-1}) decrease, many new peaks emerge. Several shoulders or peaks appear around the >C═O, ═C—O—, and —CCOC— regions. The shoulders around the >C═O peaks were identified as the >C═O stretch of a lactone at 1770 cm^{-1} and the >C═O stretch in a ketone at 1715/1708/1175 cm^{-1}, respectively.[23] The new peak at 1600 cm^{-1} suggests that the

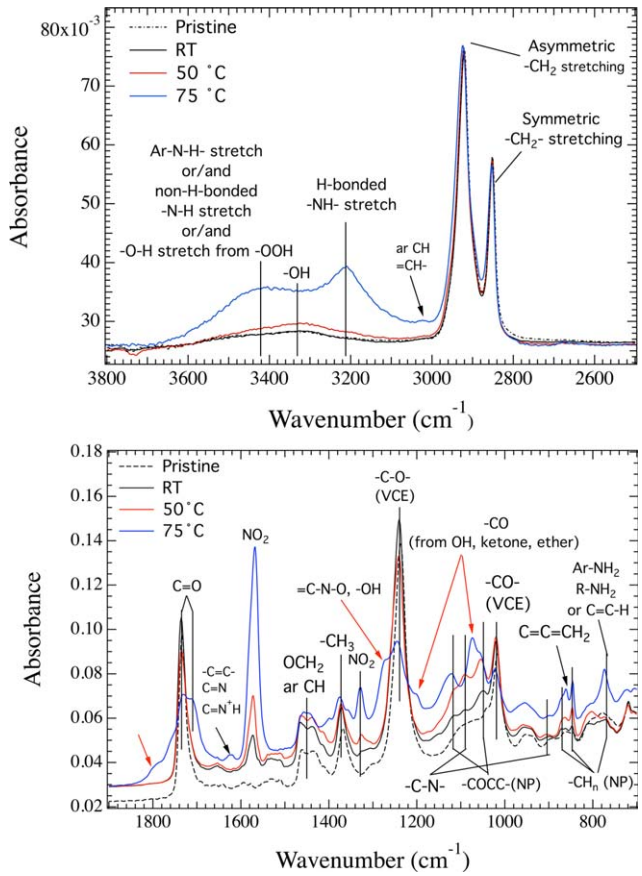

Figure 11. FTIR spectra of the EVA-OH samples before and after being exposed to NP vapor at different temperatures for 9 months. [Color figure can be viewed in the online issue, which is available at wileyonlinelibrary.com.]

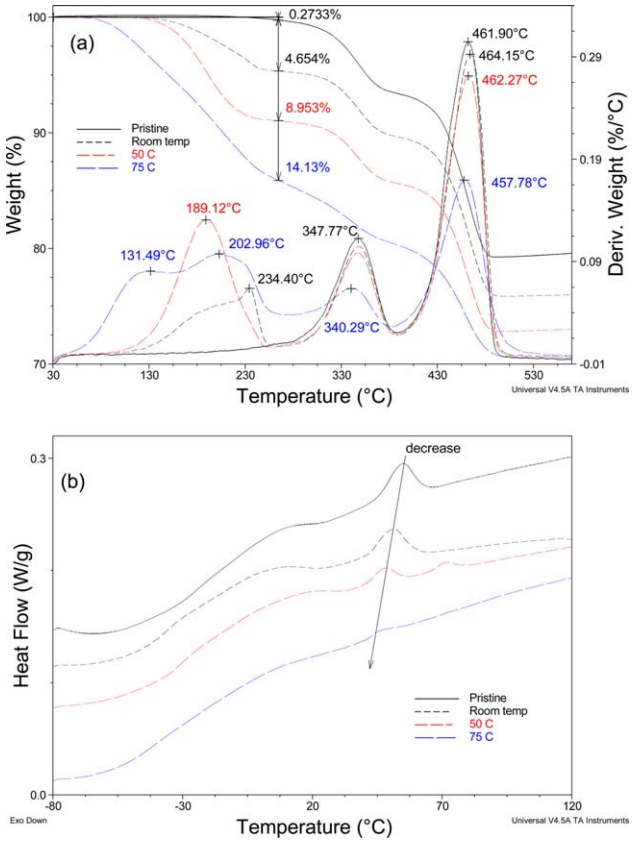

Figure 12. The effect of temperatures on the TGA (a) and DCS (b) results of the EVA-OH composites exposed to the NP vapor for 9 months. [Color figure can be viewed in the online issue, which is available at wileyonlinelibrary.com.]

formation of conjugated diene (—C=C—).[11,23] The —C—O— peak at 1040 cm^{-1}, associated with the —COO— group in the X-linker, also largely decreases. The intensities of the —C—N— peaks at 1090 and 910 cm^{-1} decrease, suggesting the —C—N— cleavage in the NP molecules. Many of the detected molecular fragments might result from the changes in —ar—NH—, —OH, —OOH, different carbonyl groups, =C—O— bands, —C=C— groups, which confirm the incision of X-linkers. Since the uncross-linked EVA-OH molecule is almost the same as EVA, the thermal degradation mechanisms of EVA under the acidic environment will dominate the EVA-OH degradation.[11,23,24,31] All of the spectral changes suggest that the irregularity of EVA-OH backbone greatly increases after the EVA-OH was exposed to NP vapor at 75°C for 9 months.

Thermal Analysis

Figure 12(a) and Table IV summarize the TGA results of EVA-OH before and after the NP vapor exposure at different temperatures. At RT, the DT_{NP} and $DT_{EVA\text{-}OH}$ features are clearly separated. Similar to the results obtained from the liquid sample (see Figure 4), NP shows one DT_{NP} (at 234.4°C) with a shoulder at the low temperature end, which may suggest the different interactions between EVA-OH and BDNPA versus BDNPF molecules. The estimated VAc content in the exposed sample is almost the same as that in the pristine EVA-OH, which suggests no significant degradation occurring at the ambient conditions. At 50°C, DT_{NP} greatly decreases from 234.4 to 189.1°C, suggesting the degradation of NP. Based on the 2nd weight loss, we estimated that the concentration of the VAc segment slightly increases though this value may also include some degraded materials. For the 75°C samples, the split DT_{NP}s confirm the significant degradation of NP. As a cascade effect, the large degradation in EVA-OH also occurs. For the liquid samples, the degraded materials, such as incised X-linkers, were extracted from the polymer into the liquid NP. In the vapor sample, except for the low boiling point materials, the degraded materials accumulate and interact with each other inside the polymer matrix. The peak at 131.5°C may be associated with the decomposition of the degraded BDNPA while the peak at 202.96°C might be associated the decomposition of the degraded BDNPF. Furthermore, DTs of degraded low MW materials and the polymer convolute together, and give a broad band between 200 and 280°C. One possible reason for this broad band is the decomposition of X-linker [methylene bis-(4-phenyl-isocyanate) (MDI) group], which decomposes at ~260°C. After the scission, MDI—a reactive agent, may react with degraded fragments from NP to form new materials. Accordingly, the greatly increased 2nd weight loss, associated with the increased VAc value, suggests that additional compounds similar to acetic acid and/or ketone are formed. On the other hand, the decreased 3rd weight loss indicates a large decrease in the mass of the ethylene segment, which confirms the severe structural changes in the backbone of EVA-OH. Upon the X-linker removal, the vinyl alcohol (VA) group forms, which is prone to be hydrolyzed under the acidic environment

Table IV. Summary of Weight Loss at Different Temperature Ranges for the EVA-OH Composites Before and After NP Vapor Exposure at Temperatures for 9 Months (Heating Rate = 10°C/min)

	Wt loss (%) at different temperature ranges				
Sample	1st <277°C	2nd 277-390°C	3rd 390-530°C	Polymer (wt %)	VAc (%)
Pristine	0.79	5.79	13.55	20.4	41.1
Room temperature	4.65	5.72	13.73	20.8	41.2
50°C	8.95	5.43	12.72	19.0	45.1[a]
75°C	14.13	5.61	9.78	16.5	56.9[a]

[a] Due to the large degradation, the weight loss between 277 and 390°C also includes some of the degraded materials, which may not be the VAc segments.

Table V. Summary of the T_g, T_m, and Heat of Fusion of the EVA-OH Samples Before and After the NP Vapor Exposure at Different Temperatures for 9 Months

Sample	T_g (°C)	T_m (°C)	H (J/g—polymer)
Pristine	−35	54.6	13.47
RT (9 months)	−37	51.1	11.57
50°C (9 months)	−38	47.9, 71.3	3.97, 1.97
75°C (9 months)	−41	46.6	2.82

below 390°C.[32] Therefore, both decreased polymer weight and hydrolyzed VA could also contribute to the increased VAc content in the 75°C sample.

Figure 12(b) and Table V summarize the DSC results of the vapor samples. Compared to T_m of the pristine sample (54.6°C), T_m of the RT vapor sample decreases to 51.1°C, which is lower than that of the corresponding liquid sample (52.7°C). Although the NP uptake in this sample is much less than that in the liquid sample, its T_g (−37°C) is also slightly lower than that of the liquid sample (−36°C). Compared to the pristine sample (13.47 J/g), the aged sample has a lower heat of fusion (11.57 J/g) as well. All of these differences are mainly due to the plasticizer effect of NP. The DSC results of the 50°C sample become more interesting because the original T_m feature splits into two. While T_m of VAc continuously decreases from 51.1 to 47.9°C, a new feature appears at 71.3°C. We suspect this new peak is associated with a new phase—the newly formed VA segment, which typically has a higher T_m than the VAc segments.[31] The hydrolysis of the VAc groups and urethane groups in the X-linkers will produce —OH group and results in more VA group in the aged samples than that in the pristine EVA-OH, which may be responsible for this new peak. As the temperature further increases to 75°C, while T_m of VAc further decreases to 46.6°C, both VAc and VA groups almost disappear. The heat of fusion of the portion at 46.6°C largely decreases to 2.82 J/g. All of these results suggest a considerable decrease in the crystallinity of the sample—due to possibly significant chain scission in the hydrocarbon bond related to the VAc and VA groups.

GPC Characterization for Aged EVA-OH and NP Samples

Figure 13 presents the M_w distributions (from DRI detector) of the pristine, vapor exposed, and liquid immersed EVA-OHs, and used NP. For the aged samples, we will only focus on the 75°C samples due to their large degradation. In Figure 13, we also include three chemical agents—hylene, MDI, and phenol as references. In general, the cured EVA-OHs have poor solubility in THF. The GPC result suggests that there are some low Mw polymer (25 K g/mol), oligomers, and phenol in the pristine EVA-OH. The two broad peaks between 17.8 and 19.6 min correspond to un-reacted X-linkers with MW higher than MDI ($M_w = 250$), which suggests that they are in the forms of partially uncapped inter-mediums.[10] If we assume that they are the hydrolyzed forms of hylene, their M_ws range from 286 to 362. For the vapor sample, we detect an appreciable amount of oligomers, a small peak with $M_w = 319$, and a large peak with $M_w > 250$. The appreciable amount of oligomers suggest that the degraded materials, with much lower M_w than the EVA-OH polymer, are due to the chain scission occurring on the backbone of EVA-OH, which is consistent with the DSC results. The small peak with $M_w = 319$ and the large peak with $M_w > 250$ might be attributed to the mixture of degraded NP and incised X-linkers, respectively. Furthermore, the vapor sample does not give much signal at the M_w higher than 50K g/mol, which suggests that the reactive species in the NP vapor cause the oxidative degradation of EVA-OH, resulting in the formation of additional cross-links in the polymer, and a decreased solubility. On the other hand, for the liquid immersed EVA-OH, we detect not only a large amount of NP, but also some polymer with a higher M_w (40K g/mol) than that found from the pristine EVA-OH. This result suggests that the immersed EVA-OH has a better solubility in THF than the pristine EVA-OH, which might be due to the removal of X-linkers during the NP immersion process. Some cured EVA-OH, therefore, becomes uncured, and hence dissolves better in THF. However, the small peak at a low M_w end ($M_w < 300$) suggests the low concentration of degraded materials, which confirms the structural changes in the liquid sample are not as significant as those in the vapor sample. This result is consistent with the results obtained from the TGA and FTIR characterization. For the used liquid NP, we detect two large peaks, which are associated with NP and the degraded materials (possibly including degraded NP and incised X-linker). Furthermore, we also detect a negative peak, which is identified as an acetic acid like materials ($M_w = 60$). Since the refractive index of acetic acid is smaller than that of THF, it gives a negative peak in the DRI detector. The result confirms the formation to acetic acid in the EVA-OH degradation process. The reason for not detecting acetic acid in the vapor sample may be due to the evaporation of acetic acid from the sample at 75°C. Similarly, if there is some acetic acid formed in the NP immersion, it was extracted out of the sample by NP.

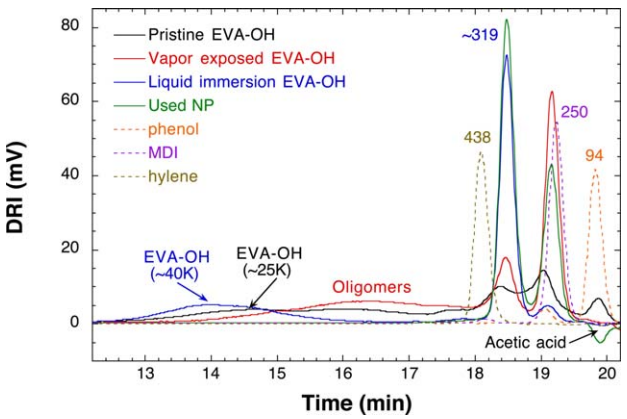

Figure 13. The GPC results (from DRI detector) of pristine (black curve), vapor exposed (red curve) and liquid immersion (blue curve) EVA-OHs, and used NP (green curve) (the aging conditions are 75°C for 9 months). M_ws of pure chemical agents are labeled near their peaks. (*To better illustrate the GPC result of the pristine EVA-OH, the intensities of other two aged EVA-OH samples were reduced by ~20%. The intensity of used NP was reduced by ~50%*). [Color figure can be viewed in the online issue, which is available at wileyonlinelibrary.com.]

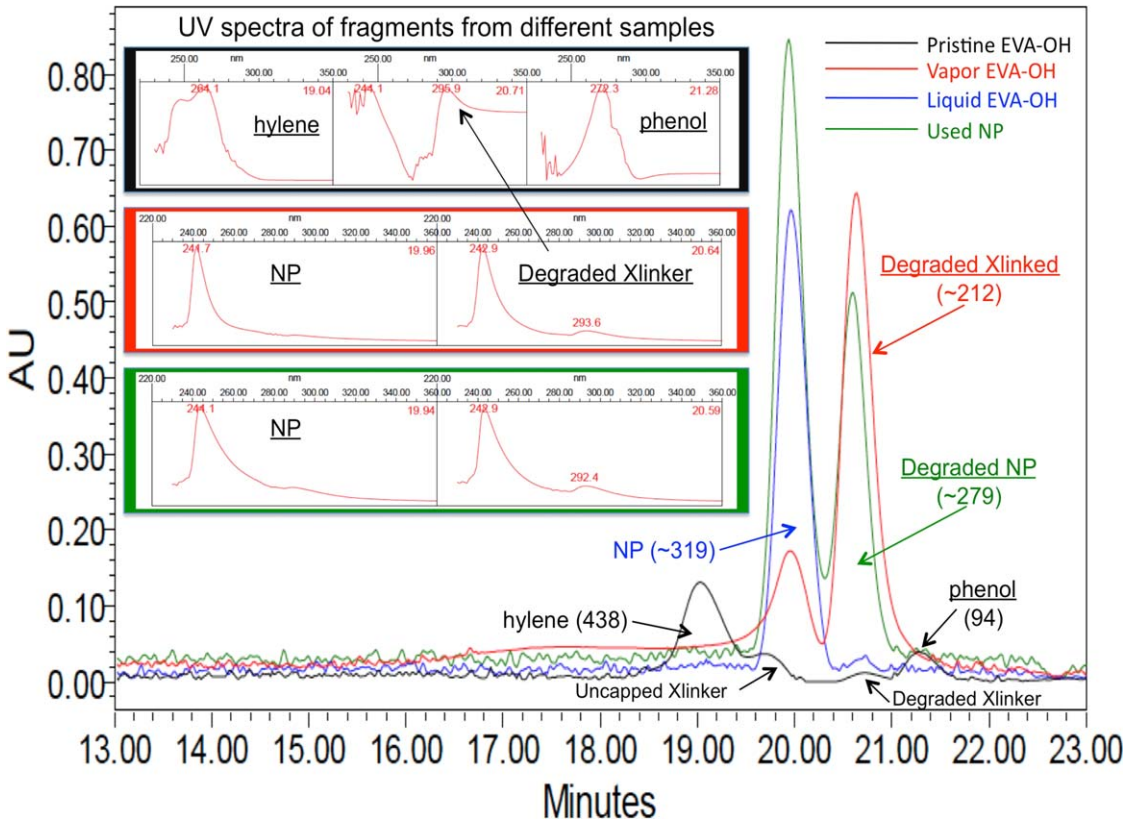

Figure 14. The GPC results (from PDA detector) of pristine (black curve), vapor exposed (red curve) and liquid immersion (blue curve) EVA-OHs, and used NP (green curve) (the aging conditions are 75°C for 9 months). Insets are the UV spectra of the eluded fragments from pristine EVA-OH (black frame), vapor exposed EVA-OH (red frame), and aged liquid NP (green frame) (the retention times of the corresponding UV spectra are labeled in the red text). [Color figure can be viewed in the online issue, which is available at wileyonlinelibrary.com.]

To further determine the chemical properties of the degraded materials in these samples, we also analyzed these fragments using PDA detectors so that their UV/vis spectra were collected, as shown in Figure 14. Unlike the DRI detector—a concentration detector, the PDA detector is a structural detector for materials that absorb in the UV/vis region. Since EVA-OH does not have a strong UV/vis absorption, plus low solubility, we barely detect the EVA-OH using the PDA detector. On the contrary, we are able to detect hylene, NP, degraded materials, and phenol. From the pristine EVA-OH, we confirm the presence of the residual hylene with a signature peak at ~264 nm together with a broad shoulder at ~245 nm, and the presence of the inter-medium products of de-capped hylene.[10] Since the de-capped hylene has a similar structure to diphenyl-amines, it gives the adsorption peak at ~295 nm. We also confirm the presence of phenol with a signature peak at 272 nm. All of these UV spectra are presented as insets in Figure 14, and grouped within the black frame. For the vapor sample, we detect two peaks with a broad shoulder at the high M_w end. The 1st peak (at ~20 min) is mainly NP, which typically gives a strong absorbance at ~238 nm in the dilute THF solution. However, the red shift on this peak (~244 nm) may be due to the influence from the dissolution of degraded materials. The second peak (~20.5 min) has a much higher intensity than the first one, which suggests that this vapor sample contains a significant amount of degraded materials. The UV spectrum of this peak contains the strong adsorption at ~243 nm, the characteristic adsorption related to $-NO_2$ group,[33] which confirms the large degradation of NP. This result is consistent with the FTIR result (in Figure 11). Furthermore, a new absorption at ~293 nm is detected, attributed to the phenyl-amine materials, such as the incised X-linker. The low intensity of this absorption is due to the initial low concentration of X-linkers in the EVA-OH composite (< 2%). From the DRI results, we know that the M_w of the degraded NP is higher than 250, which confirms that NP

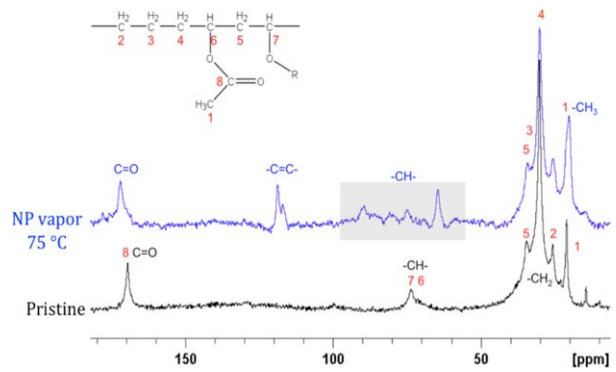

Figure 15. ^{13}C NMR results of pristine and aged EVA-OH exposed to NP vapor at 75°C for 9 months (R refers to the X-linker). [Color figure can be viewed in the online issue, which is available at wileyonlinelibrary.com.]

Table VI. Summary of Chemical Shifts in the EVA-OH Composites Before and After the NP Vapor Exposure at 75°C for 9 Months

Species	Chemical shifts (ppm)
Carbonyl carbon in *pristine* sample	169
Carbonyl carbon in *aged* sample	172 (large peak) 175.8 and 178 (small peaks)
Likely —C=C— (only for *aged* sample)	118.9 and 117.1
—CH_2—COH—CH_2— in the *pristine* sample	73.7
—CH_2—COH—CH_2— in the *aged* sample	64.7
A series of small peaks in *aged* sample	89.8 to 74.6
—CH_2— groups for both samples	34.5, 30.4, 25.9
—CH_3 groups for both samples	21.0 and a small one at 14.5

degrades mainly from —C—N— bond cleavage because M_w of the materials from the —C—C bond cleavage ($M_w < 150$) would be much lower than 250. This result supports the modeling work conducted by Pauler et al. in 2007.[3] However, a broad shoulder at the high M_w end suggests that the formation of an appreciable amount of oligomers, with some UV sensitivity, may be due to the formation of conjugated structures, such as $(—C=C—)_n$. This result is consistent with the small —C=C— IR absorption feature at 1600 cm^{-1} (in Figure 11) and also consistent with the literature results.[11,18,23,34] For the liquid immersed EVA-OH, we mainly detect NP with the minimal amount of degraded materials, which supports the slight changes in this sample. Finally, we analyze the used NP. Clearly, in addition to containing the degraded NP, it also contains some aromatic materials that give the absorption at 292.4 nm, which might come from the extraction of incised X-linkers. The incised X-linker together with other low M_w materials corresponds to the peak at 133°C in the TGA result of the used NP (see Figure 7).

^{13}C Solid State NMR for NP Vapor Exposed EVA-OH Samples

Finally, we probe the chemical changes in the aged EVA-OH samples using ^{13}C solid state NMR. Figure 15 presents the ^{13}C

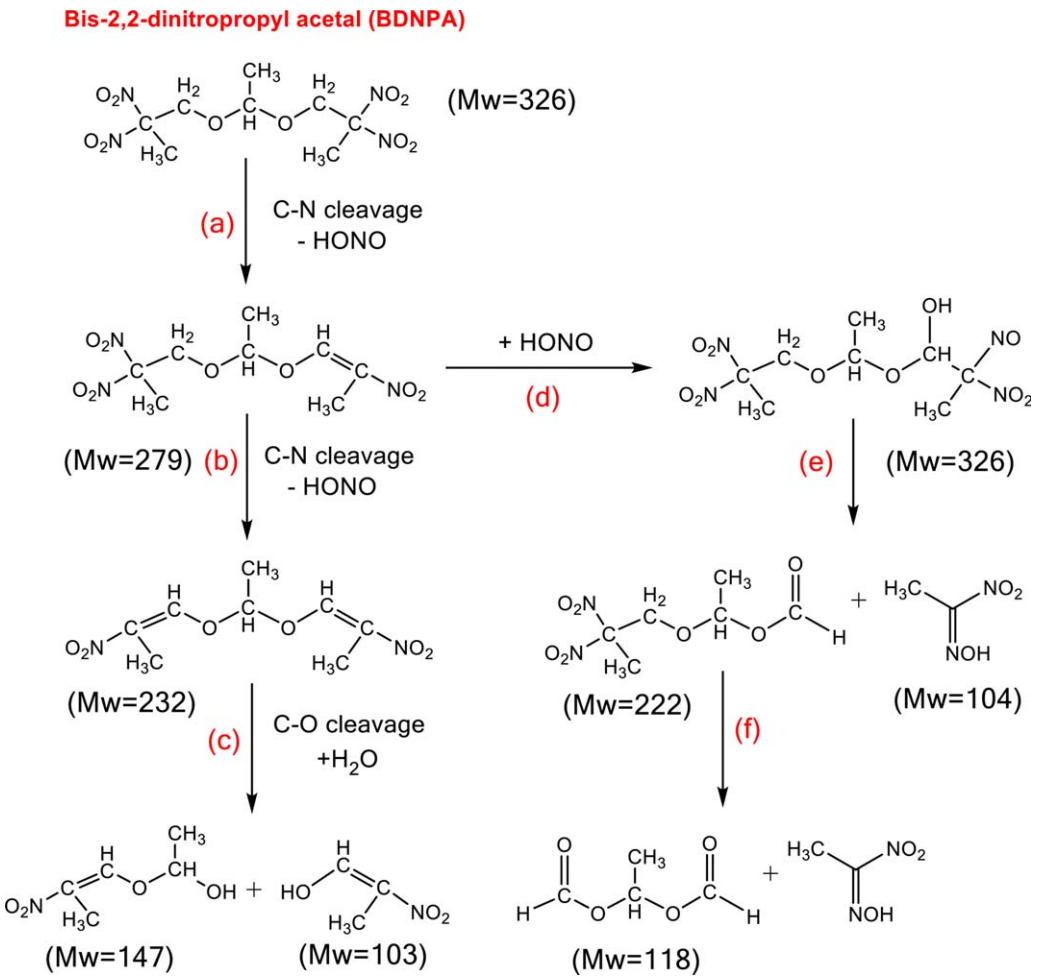

Scheme 1. The simplified degradation mechanisms of BDNPA under thermal, oxidative and/or hydrolysis conditions.[3,4] [Color figure can be viewed in the online issue, which is available at wileyonlinelibrary.com.]

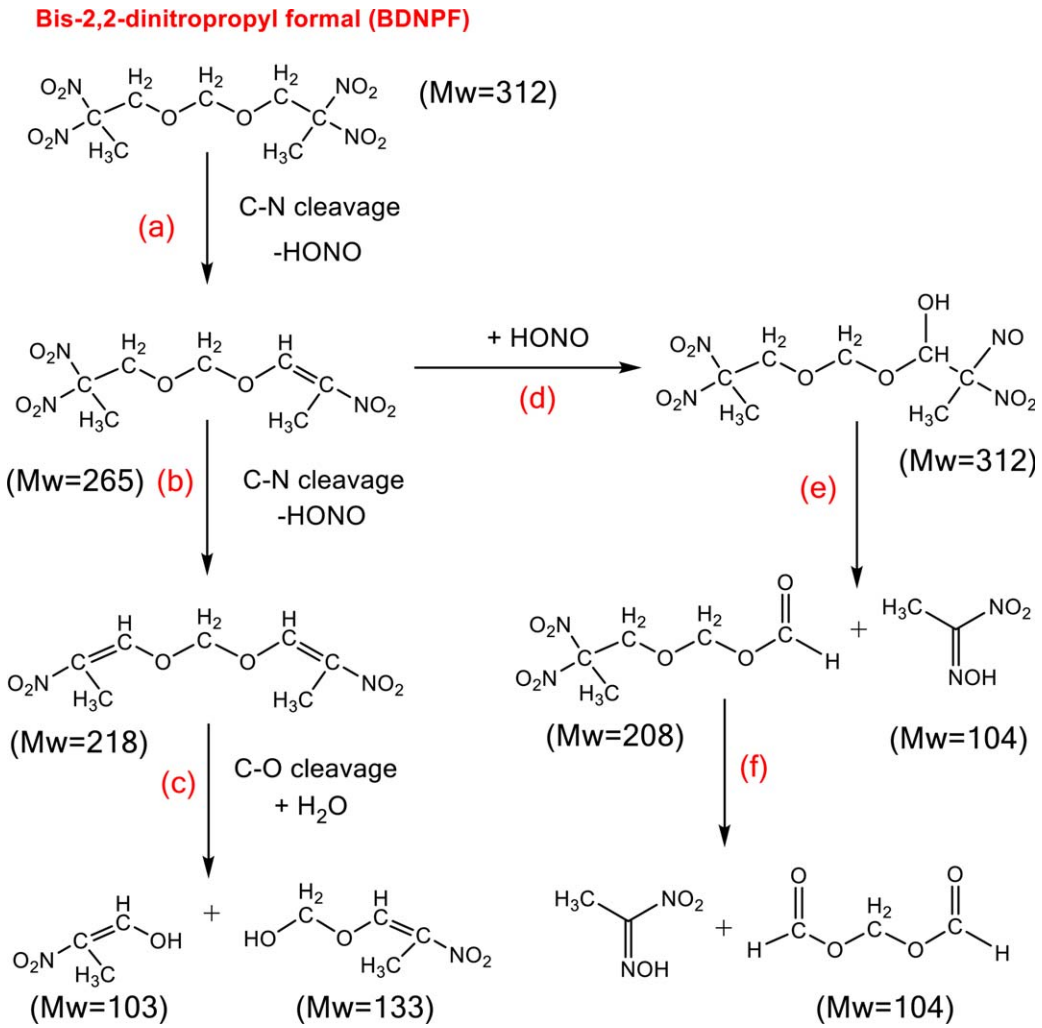

Scheme 2. The simplified degradation mechanisms of BDNPF under thermal, oxidative and/or hydrolysis conditions.[3,4] [Color figure can be viewed in the online issue, which is available at wileyonlinelibrary.com.]

NMR result of the 75°C vapor sample together with the pristine EVA-OH sample. Table VI presents the chemical shifts for the different functional groups. The NMR spectrum of the vapor sample shows a change in the chemical shift on the carbonyl resonance (labeled 8), which suggests large changes in the local environment of the carbonyl groups. Typically, when the peak broadens, the mobility of >C═O decreases. The broadened peak 8 suggests that the carbonyl groups may attach to more rigid chains. One of the new peaks at 122 ppm with a small shoulder is most likely due to the formation of different types of dienes (—C═C—). A few small new peaks between 72 and 100 ppm suggest the formation of new aliphatic carbon in the —CH— species. Accordingly, the peak broadening around peaks 5, 6, and 7 suggest large changes in the mobility of the C—O bonds attached to the aliphatic carbons. Furthermore, the peak characteristics (intensities and widths) of —CH_2— groups (labeled 2–5) noticeably change in the spectrum of the aged sample, which may be due to not only the large changes in the mobility of the C—O bonds attached to these aliphatic carbons, but also the newly formed functional groups with —CH_2—. The increased —CH_3 peak may come from more acetic acid formation through VAc hydrolysis and/or the terminated reaction though chain scission. All of these observations are consistent with the results of the other characterizations, and suggest significant degradation in the carbon skeleton in the EVA-OH sample after being exposed to the NP vapor at 75°C for 9 months.

It is worth noting that one possible factor, which may complicate this study, is the stainless steel mesh used as a support for the EVA-OH samples in the NP vapor phase. Some transition metals (Fe, Cr) in the mesh may serve as a catalyst to reduce the activation energy for the polymer degradation. Nevertheless, this comparison study concludes that the NP vapor exposure can be more detrimental to the EVA-OH polymer than the NP liquid immersion even at room temperature.

Proposed Degradation Mechanisms

In 2007, Rauch et al proposed that the initial step in the NP thermal decomposition is the NP evaporation, followed by the fragmentation of the C—O acetal/formal bond.[4] This is then followed by nitro-nitrite rearrangement and NO/NO_2 cleavage to form carbonyl species. However, their study suggests that the

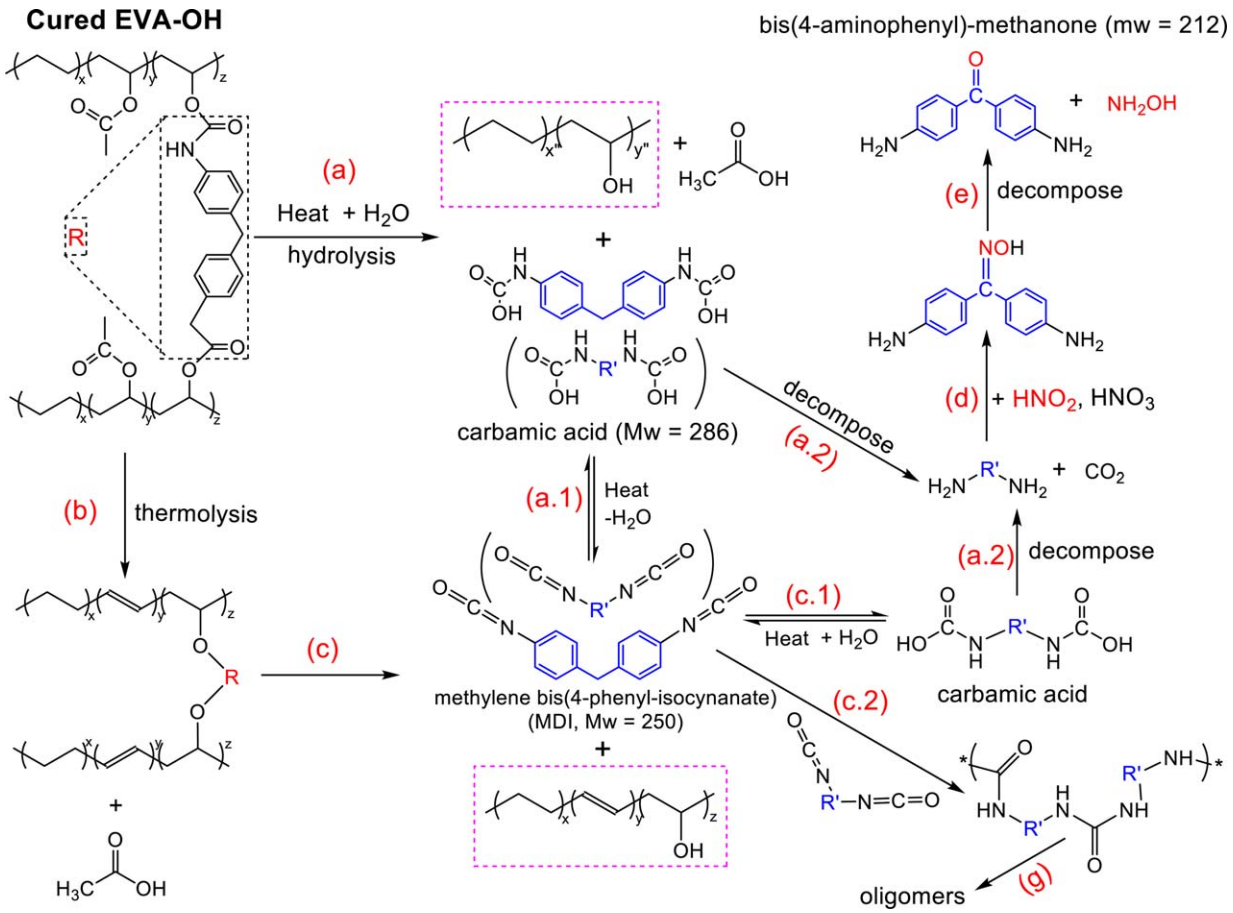

Scheme 3. Possible degradation mechanisms of the cross-linker removal and continued degradation in the EVA-OH under moisture and acidic environment.[8,10,19–23,30,35,36] [Color figure can be viewed in the online issue, which is available at wileyonlinelibrary.com.]

decomposition does not proceed until the temperature is above 160 to 180°C, which is much higher than the 75°C used here. On the other hand, the prior constituent aging studies suggest that a different decomposition mechanism may play a dominant role in the NP degradation at a low temperature (< 75°C).[5,35] The work of Pauler et al. suggests that the C—N bond scission occurs at a lower activation energy than the C—O bond scission, and eliminates HONO.[3] Pauler et al also suggest that due to the cage effect, the formed HONO can re-bond to the NP fragment before diffusing out of the liquid to form a slightly more stable R—ONO isomer of NP. However, when the HONO molecules are in the vapor phase, they can be reactive and form H_2O and NO_x species. Furthermore, when the sample is heterogeneous with a large interfacial area, the kinetics of the reaction will be enhanced. The simplified degradation mechanisms of BDNPA and BDNPF through —C—N— and —C—O— bond scission are illustrated in Schemes 1 and 2, respectively. In this study, both FTIR and GPC characterizations suggest that the majority of the degraded NP gives $M_w > 250$, which confirms the —C—N— bond scission. Evidently, the presence of oxidizing NO_x gases and moisture causes the formation of the chemical species, such as NO, HNO_2, HNO_3, H_2O and so forth, which significantly accelerate the NP and EVA-OH degradation in the NP vapor phase at 75°C. As proposed in Scheme 3, these acidic species attack the —CO— groups in the VAc segments though both hydrolysis [Scheme 3(a) and/or thermolysis Scheme 3(b)] to release acetic acid. The same hydrolysis might also occur in the urethane group in the X-linkers to form carbamic acid, which might undergo two possible reactions: Scheme 3(a.1) to form methylene bis(4-phenyl-isocynanate) (MDI), and Scheme 3(a.2) to form 4,4'-methylene bis-benzenamine (MBBA). MDI is a reactive agent and can undergo the thermal hydrolysis through Scheme 3(c.1) to generate MBBA too. Under the heat, moisture, and acidic environment, NO molecules might react with MBBA through an addition reaction through Scheme 3(d) to form bis(4-aminophenyl)-methanone-oxime. This oxime can easily decompose into bis(4-aminophenyl)-methanone and hydroxylamine through Scheme 3(e). Furthermore, MDI molecules can react among themselves to form dimers or even oligomers through Scheme 3(c.2) and (g).[10] Clearly, with many possible reaction pathways, the degradation of EVA-OH might generate many fragments with different functional groups, such as free —OH, poly—OH, —OOH, —NH_2, —NH—, ar—CH, ar—NH_2, ar—NH—, =CH— and different ketones (>C=O) groups, which cause the complicated changes in the spectra of FTIR, UV/vis, and NMR, and the results of TGA, DSC, and GPC characterizations.

We believe that the important steps in the EVA-OH degradation are the hydrolysis of the VAc group and the scission of the X-

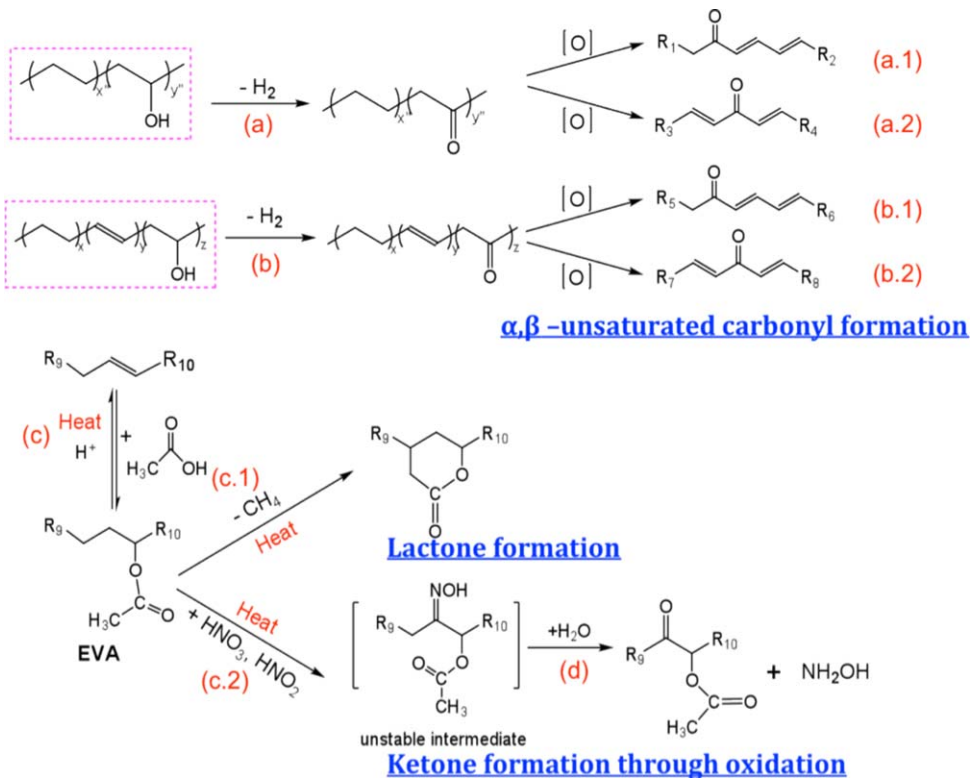

Scheme 4. The possible degradation mechanisms of degraded EVA-OH under thermal, oxidative and/or hydrolysis conditions.[8,10,19–23,30,35,36] [Color figure can be viewed in the online issue, which is available at wileyonlinelibrary.com.]

linkers. Upon the X-linker removal, the degradation of EVA-OH is very similar to that of EVA. Based on the literature,[19,20,22,23,36,37] some possible thermal degradation mechanisms are highlighted in Scheme 4. When EVA is thermally oxidized, many fragments containing >C═O and ─CO─ are formed. The cleavage of ─COOH groups and the formation of acetic acid are also well documented.[18,23,31,32,34] The deacetylation of the intermediate results in α, *β*-unsaturated carbonyl formation through Scheme 4(a)s and (b)s, which is the main cause of the yellowish color in the aged EVA.[11,23,30] The increased intensity of ─C═C─ bending at ~1600, ~850, 780 cm^{-1} in the FTIR spectrum of the 75°C sample in Figure 11 and the chemical shift at ~120 ppm in NMR in Figure 15 seem to support this hypothesis. The increased intensities of all bands in the low wavenumber region (<1000 cm^{-1}) (in Figure 11) correspond to all kinds of ─CH_n out-of-plane bending, deformation, and twisting. The formation of ─NH_2 will also contribute to some broadening of bands in this region. Accordingly, the ─CO─ peak becomes boarder at the high wavenumber end (at 1770 cm^{-1}) due to the lactone formation through the anhydration of VAc,[23] as shown in Scheme 4(c.1). The double bond formation will allow the materials to be further degraded through chain scission and cross-link with the reactive species in the NP vapor and result in the large irregular structures in the 75°C vapor sample.

CONCLUSIONS

The stability of polymer binders is a great concern in their applications where they are used in the highly filled composites. Although most polymers do not have the aging problem when they are used in the homogeneous phase, they become vulnerable when they are used in the highly heterogeneous matrix. The situation is further complicated by exposing the highly filled polymer composite to acidic and/or moisture environment. In this study, we demonstrate that the NP vapor condition, rather than the NP liquid, is detrimental toward the stability of the EVA-OH even at the relative low temperature (<75°C). It is the NP degradation that triggers the degradation of the polymer. Therefore, to minimize this cascade effect, we should minimize the NP usage. On the other hand, to improve the chemical stability of NP and EVA-OH, adding anti-oxidants will be beneficial. In further work, a more systematic and a long-term aging study will be conducted to study the kinetics of the thermal aging of the EVA-OH/filler composites under the acidic and/or humidity conditions.

ACKNOWLEDGMENTS

We thank Bruce Orler for the TGA and DSC measurements. We thank Dr. Cindy Welch, Rulian Wu, and Robert Gilbertson for the discussion on the possible reaction mechanisms. We thank John Barton (KCP) for helping with the EVA-OH material production. This work is funded by the US Department of Energy's National Nuclear Security Administration under contract DE-AC52-06NA25396.

REFERENCES

1. Salazar, M. R.; Lightfoot, J. M.; Russell, B. G.; Rodin, W. A.; McCarty, M.; Wrobleski, D. A.; Orler, E. B.; Spieker, D. A.;

Assink, R. A.; Pack, R. T. *J. Polym. Sci., Part A: Polym. Chem.* **2003**, *41*, 1136.

2. Wrobleski, D. A.; Langlois, D. A.; Orler, E. B.; Labouriau, A.; Uribe, M.; Houlton, R.; Kress, J. D. *Polymer Preprints*, **2007**, *48*, 546.
3. Pauler, D. K.; Henson, N. J.; Kress, J. D. *Phys. Chem. Chem. Phys.* **2007**, *9*, 5121.
4. Rauch, R. B.; Behrens, R. *Propel., Expl., Pyrotechn.* **2007**, *32*, 20.
5. Salazar, M. R.; Kress, J. D.; Lightfoot, J. M.; Russell, B. G.; Rodin, W. A.; Woods, L. *Propel., Expl., Pyrotechn.* **2008**, *33*, 20.
6. Wrobleski, D. A.; Langlois, D. A.; Orler, E. B.; Labouriau, A.; Uribe, M.; Houlton, R.; Kress, J. D.; Kendrick, B. In the proceeding Polymer Degrdation and Performance; American Chemical Society Symposium: Chicago, IL, **2008**; Chapter 16, p 15.
7. Salazar, M.; R.; Kress, J. D.; Lightfoot, J. M.; Russell, B. G.; Rodin, W. A.; Woods, L. *Polym. Degrad. Stabil.* **2009**, *94*, 9.
8. Brown, D. W.; Lowry, R. E.; Smith, L. E. *Macromolecules* **1980**, *13*, 5.
9. Labouriau, A.; Densmore, C.; Meadows, K.; Cordova, B.; Lewis, R. LA-UR-06–5294; Los Alamos National Laboraotry: Los Alamos, New Mexico, 2006; p 17.
10. Densmore, C.; Eastwood, E. LA-UR-06-6812; Los Alamos National Laboraotry: Los Alamos, New Mexico, 2006; p 52.
11. Létant, S. E.; Plant, D. F.; Wilson, T. S.; Cynthia, T.; Alviso, C. T.; Read, M. S. D.; Maxwell, R. S. *Polym. Degrad. Stabil.* **2011**, *96*, 10.
12. Wilson, P. M. KCP-613-6004; KCP of AlliedSignal: Kansas City, MO, **1997**; p 17.
13. Eastwood, E. A. KCP-613-8161; KCP of Honeywell: Kansas City, MO, 2006; p 34.
14. Fletcher, M.; Powell, S. LANL internal report; Los Alamos National Laboraotry: Los Alamos, New Mexico, 2003, p 10.
15. Gottlieb, L.; Bar, S. *Propel., Expl., Pyrotechn.* **2003**, *28* (1), 6.
16. Yang, D.; Pacheco, R.; Henderson, K.; Hubbard, K. M.; Devlin, D. *J. Appl. Polym. Sci.* **2014**, *131*, 40729.
17. Thompson, D. G.; Deluca, R. LA-CP-14-00015; Los Alamos National Laboratory: Los Alamos, New Mexico, 16, 2013; p 20.
18. Gilbert, J.; Kipling, J. *Fuel* **1962**, *12*, 11.
19. McNeill, I. C.; Jamieson, A.; Tosh, D. J.; McClune, J. J. *Eur. Polym. J.* **1976**, *12*, 8.
20. Smith, R. M.; Baker, G. K.; Smith, C. H. In Chemistry and Properties of Crosslinked Polymers, Labana, S. S., Ed.; Academic Press, Inc. (Elsevier): New York, **1977**; p 8.
21. Smith, R. M.; Baker, G. K.; Smith, C. H. Thermal Aging of Cured Ethylene/Vinyl Acetate and Ethylene/Vinyl Acetate Alcohol Elastomers; Proceeding in ACS Symposium on Chemistry and Properties of Crosslinked Polymers, S.S. Labana, San Francisco, 1976, p175.
22. Perez, E.; Lujan, M.; Salazar, J. M. D. *Macromol. Chem. Phys.* **2000**, *201*, 6.
23. Allen, N. S.; Edge, M.; Rodriguez, M.; Liauw, C. M.; Fontan, E. *Polym. Degrad. Stabil.* **2001**, *71*, 14.
24. Khan, N.; Patel, M.; Pitts, S.; netherton, D.; Monks, P.; Robinson, M.; Morrell, P. In Pacifichem Conference, ACS, Honolulu, HI, **2010**.
25. Salazar, M. R.; Thompson, S. L.; Laintz, K. E.; Meyer, T. O.; Pack, R. T. *J. Appl. Polym. Sci.* **2007**, *105*, 1063.
26. Eastwood, E. A. KCP-613–6929; Kansas City Plant: Kansas Ciy, MO, 2004; p 72.
27. Shen, S.-M.; Leu, A.-L.; Yen, H.-C. *Thermochimica Acta* **1991**, *176*, 13.
28. hen, S.-M.; Chang, F.-M.; Hu, J.-C.; Leu, A.-L. *Thermochimica Acta* **1991**, *181*, 12.
29. Hammer, C. F. *Marcomolecules* **1971**, *4*, 3.
30. Wypych, G. Handbook of Plasticizers, 2 ed.; ChemTec Publishing, Toronto: **2012**; p 800.
31. Patel, M.; Pitts, S.; Beavis, P.; Robinson, M.; Morrell, P.; Khan, N.; Khan, I.; Pockett, N.; Letant, S.; II; G. V. W.; Labouriau, A. *Polym. Test.* **2013**, *32*, 9.
32. Gilman, J. W.; VanderHart, D. L.; Kashiwagi, T. In Fire and Polymers II, Materials and Test for Hazard Prevention; ACS Symposium Series 599: Washington, DC, **1994**; Chapter 3, p 25.
33. Zhang, J.; Yang, C.; Wang, X.; Yang, X. *Analyst* **2012**, *137*, 7.
34. Grassie, N. *Trans. Faraday Soc.* **1952**, *48*.
35. Kress, J. D.; Wrobleski, D. A.; Langlois, D. A.; Orler, E. B.; Lightfoot, J. M.; Rodin, W. A.; Huddleston, C.; Woods, L.; Russell, B. G.; Salazar, M. R.; Pauler, D. K. Proceeding of Polymer Degradation and Performance, ACS symposium series 1004: Washington DC, 2009; chapter 20, p 227.
36. Costache, M. C.; Jiang, D. D.; Wilkie, C. A. *Polymer* **2005**, *46*, 12.
37. Riva, A.; Zanetti, M.; Braglia, M.; Camino, G.; Falqui, L. *Polym. Degrad. Stabil.* **2002**, *77*, 6.